PAPER • **OPEN ACCESS**

Finite element analysis of thermal sensitivity of copper nanorods, nanoellipsoids, nanospheres and core-shells for hyperthermia application

To cite this article: Muhammad Usama Daud *et al* 2024 *Mater. Res. Express* **11** 035004

Materials Research Express

PAPER

Finite element analysis of thermal sensitivity of copper nanorods, nanoellipsoids, nanospheres and core-shells for hyperthermia application

Muhammad Usama Daud[1], **Ghulam Abbas**[1], **Muhammad Afzaal**[1], **Muhammad Qamar**[1], **Muhammad Yasin Naz**[2], **Muhammad Irfan**[3], **Saifur Rahman**[3], **Abdul Ghuffar**[1] and **Muawia Abdelkafi Magzoub Mohamed Ali**[4]

[1] Department of Physics, Riphah International University Faisalabad Campus, Pakistan
[2] Department of Physics, University of Agriculture Faisalabad, 38040 Faisalabad, Pakistan
[3] Electrical Engineering Department; College of Engineering, Najran University Saudi Arabia, Najran 61441, Saudi Arabia
[4] Sudan Technological University, Electrical & Electronics Engineering Department, Al Iza'a St, Omdurman 13315, Sudan

E-mail: muawia.magzoub@nu.edu.sd

Keywords: hyperthermia, copper nanostructures, thermal response, core-shell structures, heat transfer, COMSOL multiphysics, volume coverage ratio

OPEN ACCESS

RECEIVED
9 December 2023

REVISED
10 March 2024

ACCEPTED FOR PUBLICATION
18 March 2024

PUBLISHED
28 March 2024

Abstract

Hyperthermia is a cancer treatment strategy that involves raising the temperature of the afflicted tissues without disrupting the surrounding tissues. This study is focused on finite element analysis of copper, nanoellipsoids, nanorods, nanospheres and core-shells for potential hyperthermia application. The temperature of copper nanostructures was elevated using an external source to the desired temperature to destroy the cancerous cell. The COMSOL Multiphysics package was used to calculate how long it would take to achieve the desired temperature using different nanostructures of copper. Thermal sensitivity of the tested nanostructures was checked by putting them in a spherical domain of tissue. It was observed that copper nano-rod attained the highest temperature of 43.3 °C compared to other geometries. It was also found that these geometries attained thermal equilibrium just after 0.5 μs. However, the copper nano-ellipsoid had a higher core volume, which is utilized to determine the thermal sensitivity of the nanostructures. Noble metal (Au) coating was first found to be better than PEG polymer coating for investigating core–shell structures. The Au coating on the surface of the copper core resulted in a gradual decrease in temperature with an increasing volume coverage ratio. These results conclude that copper nanostructures can be suitable candidates for hyperthermia.

1. Introduction

Hyperthermia (HT) is a type of cancer treatment in addition to chemotherapy, radiation, surgery, immunological and gene therapy [1]. HT is used in oncology to elevate tissue temperature and kill or hinder cancer cell growth by using an external heat source [2]. The word 'hyperthermia' refers to a variety of heat application procedures that are used in conjunction with other cancer therapies (especially radiotherapy and chemotherapy) [3]. Although most research has revealed that high temperatures directly damage malignant cells [4] and sensitize them to various treatment modalities, they supplement chemotherapy and radiation therapy while causing little or no damage to normal cells [5]. Consequently, HT has found widespread application as an adjuvant therapy in cancer management [6, 7], as depicted in figure 1. It is important to note that while hyperthermia can stand alone as a potent inducer of cancer cell death, its collaborative potential with conventional therapies accentuates its role in comprehensive treatment regimens. The intricate interplay between HT, chemotherapy, and radiotherapy warrants detailed exploration to optimize therapeutic outcomes.

Hyperthermia (HT) treatment involves raising tissue temperatures within the range of 39 °C–48 °C for extended durations [6]. Different temperature thresholds define specific outcomes: temperatures beyond 50 °C result in coagulation, 60 °C–90 °C lead to thermal ablation, and temperatures surpassing 200 °C cause charring

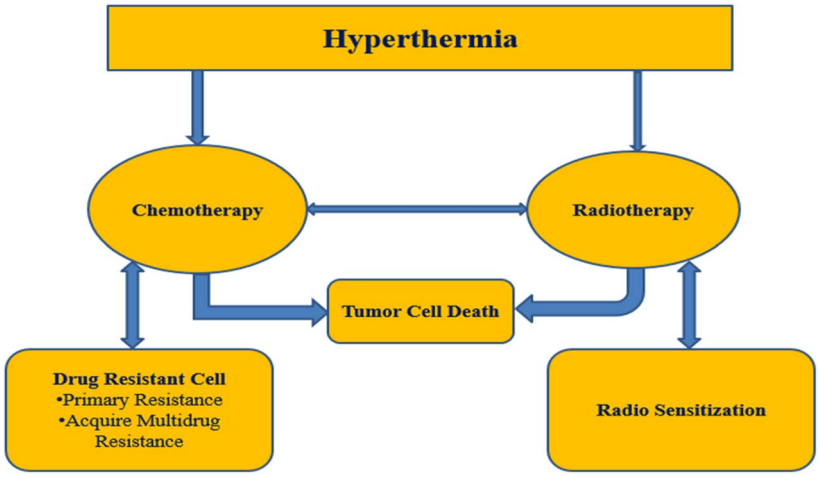

Figure 1. Working of hyperthermia in conjunction with recognized cancer therapies.

[5]. Ablation, also referred to as high-temperature treatment (HT), encompasses the direct application of chemical or thermal therapies to achieve significant tumor removal [8]. While nanoparticles hold promise in HT, their applications are still under investigation, offering potential solutions to existing challenges [11]. Although the underlying mechanisms are not fully understood, normal tissues exhibit greater thermal tolerance than cancer cells [9–11]. Patient-specific factors such as tumor location (superficial or deep-seated) and malignancy stage influence the clinical approach to HT [12].

Localized HT methods are tailored to specific scenarios. Ultrasounds, radiowaves, or microwaves are employed for small, accessible tumors [13]. Thermally conductive applicators, like current sheets and waveguides, aid in localized heat transfer, accompanied by water boluses to maintain skin temperature [4]. In local perfusion HT, heated chemotherapeutic agents are introduced into the peritoneal cavity [14]. Regional Hyperthermia (RHT) encompasses diverse approaches, including peripheral applicators and extracorporeal methods [15–19]. Successful RHT employs dipole antennas generating RF or microwave radiations to target tissues [15]. Whole-body hyperthermia (WBHT) involves extracorporeal technologies or radiation to elevate body temperature [6, 16–18]. The unfolded protein response triggered by rising tissue temperature has implications for tumor-specific antigens and immune cell recognition [20–22].

Hyperthermia induced using nanoparticles is explored through various techniques [23–26]. Nanoparticles are localized to tumors and then exposed to external energy, creating region-specific hyperthermia [24]. In the realm of hyperthermia applications, the pioneering work of Naomi Halas has significantly shaped the landscape, particularly through her investigations into core–shell nanoparticles. These novel composite spherical nanoparticles, characterized by a dielectric core enveloped by a thin metallic shell, notably gold, exhibit exceptional optical and chemical attributes suitable for both biomedical imaging and therapeutic endeavors [27, 28]. By meticulously tailoring the relative dimensions of the core and shell, these nanoparticles can achieve precise optical resonance modulation across a wide spectrum, spanning from near-UV to mid-infrared regions [29]. Notably, this spectral range aligns with the near-infrared (NIR) wavelength window, capitalizing on enhanced tissue transmissivity. Beyond their tunability, nanoshells offer advantages over conventional organic dyes, boasting superior optical properties and heightened resilience to chemical and thermal denaturation [30]. Moreover, Halas's work elucidates how the same conjugation techniques used for gold colloid can be seamlessly adapted to nanoshells, thereby expediting their integration into diverse applications. The field of core–shell nanoparticles, particularly metal nanoshells, has gained attention for their potential in various applications, including biomedical imaging and therapy. Metal nanoshells, consisting of a dielectric core covered by a thin metallic shell, offer tunable optical properties and surface characteristics, enhancing biocompatibility and functionalization. Notably, Naomi Halas' pioneering work showcases the revolutionary concept of inductive coupling, enabling remote electronic control over DNA hybridization through metal nanocrystals and a radio-frequency magnetic field. This technique allows reversible denaturation of DNA with minimal impact on surrounding molecules, opening avenues for precise manipulation of biological processes at the molecular level. This breakthrough complements Kimberly Hamad-Schifferli's contributions, demonstrating the potential of nanocrystals for optical control and manipulation of biomolecules. Hamad-Schifferli's research has implications in diagnostics, molecular imaging, and therapeutics. Together, these advancements underscore the significance of nanoparticle properties for targeted biomedical applications, highlighting the need for comprehensive exploration in diverse therapeutic and diagnostic contexts [31].

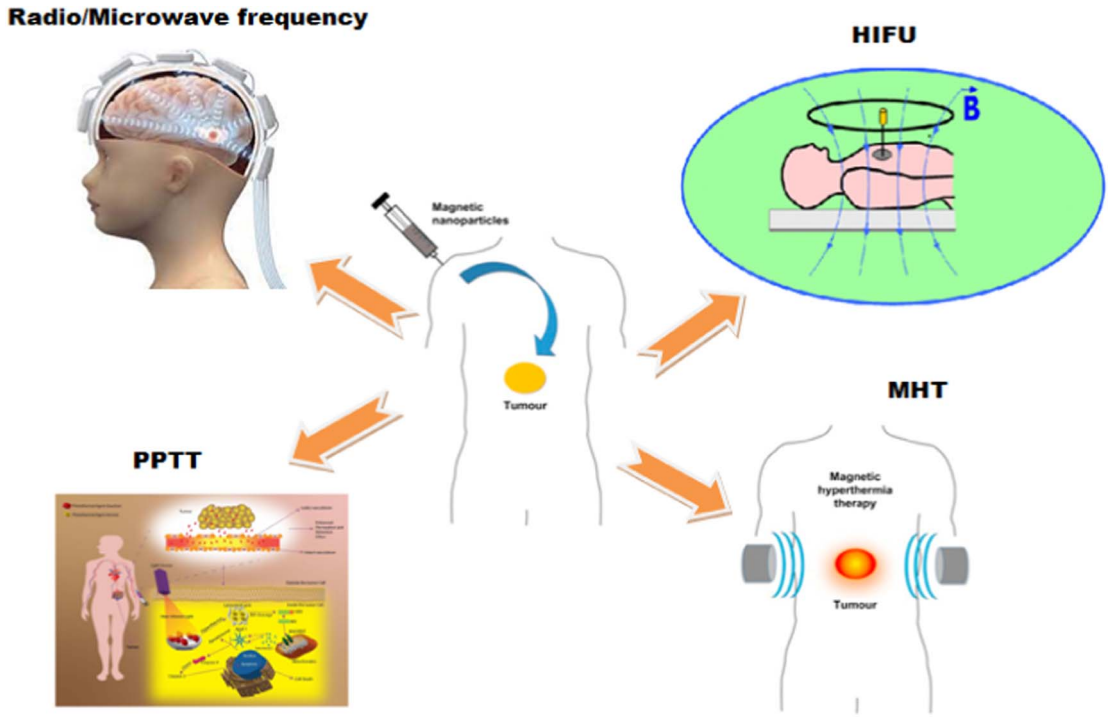

Figure 2. Illustration of techniques used for heating the nanoparticles.

Core–shell nanomaterials and nanostructures have gained significant attention due to their potential applications in various fields, notably in the transportation of bioactive compounds [32, 33]. These nanocomposites come in diverse core and shell thicknesses, sizes, and surface morphologies, ranging from stars and cubes to rods and spheres. Through methods like thin-layer deposition and functional conjugation, their surface characteristics can be tailored for improved properties compared to non-functionalized particles.

Particularly noteworthy are singular core–shell nanoparticles (NPs), offering a wide range of therapeutic applications in biotechnology, including diagnostics, tumor therapy, and drug delivery. Figure 2 illustrates some techniques used for heating the nanoparticles. These versatile structures encompass various forms, such as metallic, non-metallic, and polymeric cores and shells, each customizable to optimize desired qualities [34, 35]. One promising application of core–shell models is in specific target antitumor treatments. By enabling the controlled release of active agents within cancer tissues, these models minimize harm to healthy tissues and exert a potent influence on malignant cells. This systematic approach holds potential for tackling tumor cells that have developed resistance to hypoxia as a result of previous anti-cancer treatments.

Both human and animal metabolic activities necessitate copper, which plays pivotal roles in connective tissue cross-linking, iron and lipid metabolism [36]. However, caution is warranted as high exposure to copper can pose risks [37, 38]. Copper exhibits distinctive physical and chemical attributes, rendering it a versatile candidate for various applications [39, 40]. While its exceptional thermal and electrical conductivity, along with malleability, contribute to its versatility, copper's interaction with organic compounds can disrupt physiological and environmental processes. Despite being often considered 'inert' due to its resistance to dissolution in acids without an oxidizing agent, ionic copper (Cu^{1+} or Cu^{2+}) can form bonds with diverse organic molecules, potentially altering regular processes [41]. Notably, various cupric forms of copper can be toxic to biological systems.

Addressing potential toxicity concerns is crucial when considering the application of copper nanoparticles in hyperthermia. To mitigate these challenges, various strategies can be employed. Tailoring the size and surface characteristics of copper nanoparticles offers the potential to influence their interactions and reduce toxicity [42]. Surface modifications provide a viable means to enhance biocompatibility and minimize adverse effects. Encapsulation within biocompatible matrices or coatings acts as a protective barrier, reducing direct interactions with biological systems and diminishing toxicity risks. Implementing targeted delivery methods ensures nanoparticles are directed precisely to tumor sites, minimizing exposure to healthy tissues and mitigating potential adverse effects. Rigorous biocompatibility studies, encompassing *in vitro* and *in vivo* investigations, yield insights crucial for the prudent application of copper nanoparticles in hyperthermia treatments [43]. Optimizing nanoparticle dosage strikes a balance between therapeutic efficacy and potential

toxicity. Adhering to regulatory guidelines and safety standards is essential to safeguard patient well-being and minimize risks associated with nanoparticle-induced toxicity [42].

The features of crystalline and/or amorphous core–shell structures and their medicinal applications are unique. Small gold colloids are gradually deposited onto the surface of cores using the Stöber process [44]. The AuNPS then grow and aggregate, forming incomplete and rough covering that finally builds a continuous entire shell that completely covers the core. Daud *et al* [45] and Abbas *et al* [46] used noble metal nanoparticles (Ag and Au) to investigate the distribution of the temperature in the tumor theoretically. According to the findings, the stable temperature was achieved in 0.3 microseconds. Silver nano-rods attained the required temperature faster than other forms. However, the core volume of silver nano-ellipsoids was the largest. The current work intends to use CuNPs to obtain the necessary temperature in a shorter amount of time.

A comparative examination on heat generation is carried out in the given research using a single copper nanoparticle with diverse forms such as nanorod, nanoellipsoid and nanosphere. The volume of the above-mentioned shapes is defined as $V_{sphere} \cong V_{rod} \cong V_{ellipsoid}$ *i.e.*, $V_{sphere} = \frac{4}{3}\pi r^3 = 33510.32\ \text{nm}^3$, $V_{ellipsoid} = \frac{4}{3}\pi abc = 33401.41\ \text{nm}^3$, $V_{rod} = \frac{4}{3}\pi r^2(r+h) = 33324.96\ \text{nm}^3$. This model accounts for the thermal consequence of heat spread in tumour cells and the transient heat distributions after therapy. Alternative coating materials, such as Polyethylene Glycol (PEG) Polymer and Gold (Au), are also investigated. The thickness of the shell has been identified as an important factor influencing the thermal response of the treatment system via the thermal characteristics of the materials which are being used. Lastly, different NPs are used to replicate a thin surface layer on the core surface.

In this study, we presented a novel exploration into the hyperthermic applications of copper nanoparticles, specifically nanoellipsoids, nanorods, nanospheres, and core shells. Our research is focused on copper nanoparticles, extending beyond traditional materials like gold and silver in hyperthermia studies. Leveraging the computational capabilities of COMSOL Multiphysics, we conducted a detailed finite element analysis to investigate the thermal sensitivity of these copper nanostructures. Notably, our work includes a comparative analysis with previous studies on gold and silver nanoparticles, providing insights into the distinct thermal behavior of copper nanoparticles. A key innovation lies in our exploration of core–shell structures, examining the effect of coatings, such as gold and PEG polymer on the hyperthermic properties of copper nanoparticles. We further delved into the anisotropy of coating surfaces and investigated how varying coating thickness impacts heat sensitivity. The findings of this study not only contribute to the understanding of copper nanoparticles in hyperthermia but also extend to potential biomedical applications. This research introduces valuable insights into the thermal dynamics of copper nanostructures, paving the way for their consideration in cancer treatment strategies.

2. Method

To investigate the temperature response of cancerous tissues using nanostructures as heating sources, COMSOL Multiphysics was employed. The study aimed to address heat exchange mechanisms within tissues using distinct nanostructures, including nano-rods ($L_{cyl} = 73$ nm, $R_{cyl} = R_{cap} = 11$ nm) nano-ellipsoids (12–15–44.3 nm), nano-spheres ($R = 20$ nm), and core–shell structures. Estimating heat energy exchanges in distinct biochemical tissues is difficult due to variances in tissue function and structure. The importance of a heat transfer mechanism, the time frame of the stored energy, and variations in boundary and starting circumstances all impact energy balance [46]. Simplifying assumptions are usually necessary to reproduce essential properties of the organism's thermal condition (or its components), as well as the effects of the boundary and beginning circumstances. As the first stage in creating such models, the energy conservation equation is frequently applied to a control volume.

$$Q_{gain} = Q_{storage} + Q_{loss} + W \tag{1}$$

Key parameters included heat gain by the tissue (Q_{gain}), heat storage in tissue ($Q_{storage}$), work generated by tissue (W), and heat loss by conduction (Q_{loss}). The typical heat transfer equation for living animals is the bio-heat transfer equation. We explore its contents and assumptions by analyzing size and dimensions. This might differ based on the limitations given by the simulated item as well as the involvement of the related transport method. The Fourier heat equation may be used to anticipate the temperature distribution within cancerous cells.

$$\rho C_p \frac{\partial T}{\partial t} + \rho C_p u.\nabla \quad T + \nabla_{.q} \quad = Q + Q_{bio} \tag{2}$$

Heat flux due to conduction (q) and contributions from blood perfusion and metabolic activity (Q_{bio}) were considered.

$$q = -k\nabla \quad T \tag{3}$$

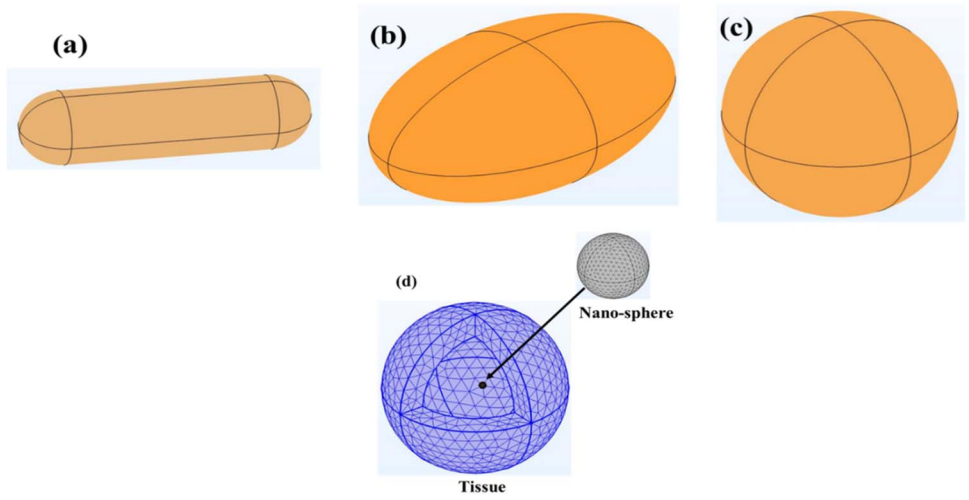

Figure 3. Different simulation morphologies (a) nano-rod, (b) nano-ellipsoid, (c) nano-sphere and (d) geometry discretization (NP embedded in tissue).

$$Q_{bio} = \rho_b C_{p,b} w_b (T_b - T) + Q_{met} \tag{4}$$

In which ρ_b is blood density which is 1000kg/m^3, k is cell thermal conductivity, ρ is tissue density, C_p is specific heat capacity of tissue at constant pressure, C_b is blood' specific heat its value is 4180J/(kg*K), T_b is blood temperature of arterial which is nearly equal to the temperature of the body (37 °C) [47], ω_b is blood perfusion rate of value 6.4*10^{-3}1/s, $Q_{met} = 5790 W/m^3$ for cancerous cell [48], T is the ambient temperature, while $Q = 10^{16}(W/m^3)$ is heat dissipated by NP in the volume of cell [49] and Q_{ext} is the heat by loss of powers. At first, it was considered that the tissue temperature was average for the body, ($T_i = 37$ °C).

$$T_i(r, 0) = T_{i0}, \frac{\partial T_i(r, 0)}{\partial t} = 0 \quad where \quad i = 1, 2 \tag{5}$$

Tissue and NP geometry were distributed on all domains assuming free tetrahedral components. There were 60246 meshing domain elements after meshing the geometry (tissue and NP), with the elemental size set to finer. The procedure's boundary conditions were as follows:

(i) The tumoral receives the whole heat flow from the nanoparticle, this is continuity.

(ii) At T = T_0 = 37 °C, the outer tissue surface is preserved.

2.1. Simulation setup and parameters

A detailed simulation setup was established, wherein nanoparticles were precisely placed within a 0.5 μm cancerous tissue area. COMSOL Multiphysics generated spatiotemporal temperature distributions, meticulously capturing the intricate interplay between nanostructures and tissue. Various copper nanostructures (nanospheres, nanorods, Core shell and nanoellipsoids) were examined, each with distinct geometries influencing heat transfer dynamics figure 3.

Further exploration involved variations in coatings, with a focus on gold and PEG polymer coatings. The impact of coating thicknesses (ranging from 5 to 40 nm) on thermal behavior was systematically studied. Simulations encompassed different coating surfaces, including spherical and ellipsoidal coatings on a copper nanoparticle core. The simulation of the formation of AuNPs shell on a copper nanoparticle core is shown in figure 4. The nanoparticles are intentionally distributed on the core in a strategic manner to emulate realistic scenarios, ensuring a more accurate representation of physical interactions. Unlike random or arbitrary placement, our distribution method enhances the reliability of the simulations, influencing temperature distributions within the tumor model. This approach is crucial, as it contributes to the robustness of our findings, aligning with our commitment to providing accurate and meaningful insights into the thermal behavior of copper nanoparticles in hyperthermia applications. Table 1 displays the thermal characteristics of the various materials utilized in this experiment.

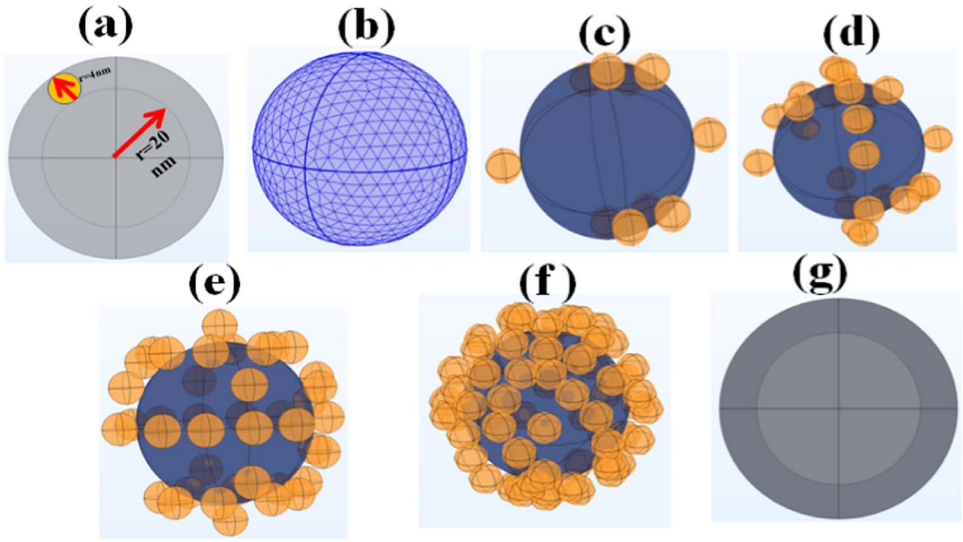

Figure 4. A shell structure was modelled in COMSOL Multiphysics as (a) a bare core with a radius of 20 nm and AuNPs with a radius of 4 nm adhered to core. (b) core (0 NP), (c), (d), (e), (f) core with 10, 25, 50, and 70 nanoparticles, and (g) full shell (100 NPs).

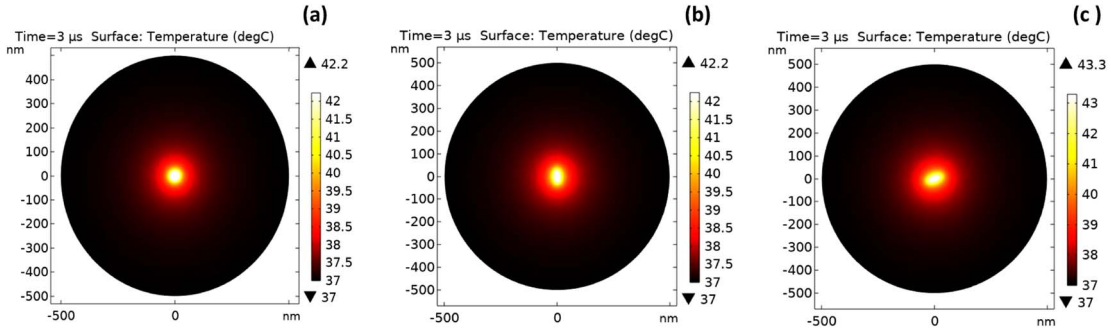

Figure 5. The two-dimensional spatial temperature distribution of a 0.5 μm tumoral cell from the start of the heating process using (a) copper nano-ellipsoid, (b) copper nano-sphere, and (c) copper nano-rod. (x-axis: radial distribution, y-axis: temperature bar).

Table 1. Material properties used in this work.

	Living Tissue [50]	Gold [51, 52]	Copper [53]	Polymer [51]
Thermal Conductivity ($Wm^{-1}K^{-1}$)	0.512	317	391	0.2
Mass Density (Kgm^{-3})	1000	19,300	8940	1000
Heat Capacity Specific ($Jkg^{-1}K^{-1}$)	3800	129	380	1000

3. Results and discussion

3.1. Temperature distribution and hyperthermia effects of copper nanostructures

Expanding our investigations to copper nanoparticles, we examined their potential application in hyperthermia therapy. Similar to our prior studies on gold and silver nanoparticles [44, 45], we introduced copper nanorods, nanoellipsoids, and nanospheres into a tumor model with a spherical shape and a 500 nm radius. The heating effects of these copper nanostructures were simulated to assess their hyperthermia-inducing capabilities.

Echoing our observations from previous studies, the initial simulation revealed the maximum temperatures achievable within the tissue using external heating, as depicted in figure 5 which is radial distribution along x-axis. The two-dimensional spatial temperature distribution of a 0.5 μm tumoral cell from the start of the heating process using copper nano-ellipsoid is showin in figure 5(a). The spatial temperature distribution of copper nano-sphere is shown in figure 5(b) while, spatial temperature distribution of copper nano-rod is shown in figure 5(c). The copper nanorod emerges as the superior geometry in achieving high temperature compared to

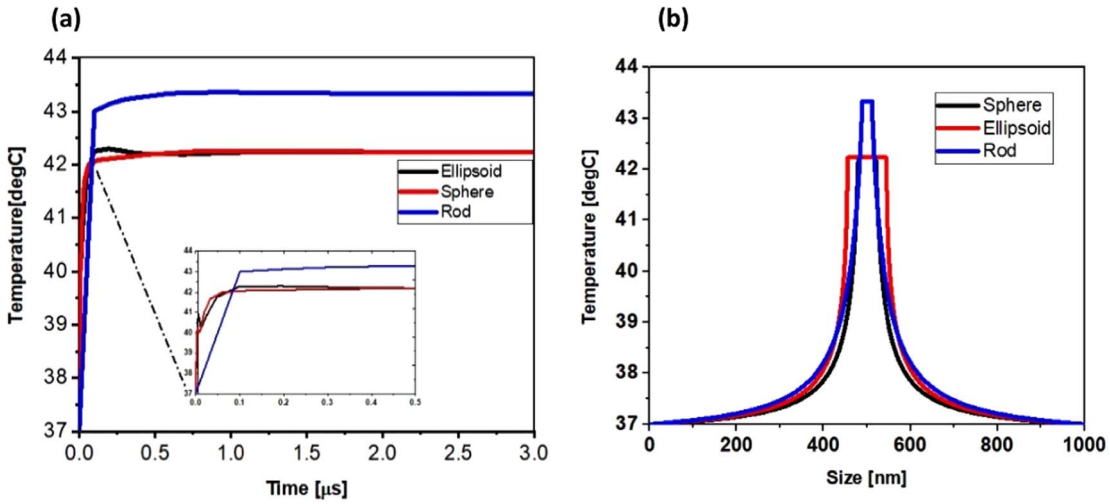

Figure 6. (a) Temperature progression at the tumor core (x = 0) and (b) after 3 micro-seconds radial distribution of therapy for three distinct types.

nanoellipsoids and nanospheres, and this can be attributed to its distinctive elongated structure. The nanorod's high aspect ratio enhances the surface area, facilitating more efficient heat absorption from the external source. Its long shape enables effective heat transfer, resulting in a uniform distribution of absorbed heat and a notable temperature increase. Enhanced thermal conductivity ensures rapid heat propagation within the nanorod. Optimized spatial distribution and orientation contribute to its effective interaction with the external heat source. The nanorod's potential for a reduced thermal equilibrium time further underscores its efficiency in attaining and maintaining elevated temperatures, making it a standout candidate for hyperthermia applications. Just as with gold and silver nanoparticles, the heating of copper nanoparticles induced changes in temperature and thermal equilibrium of the tumoral cell over time, as illustrated in figure 6(a).

3.2. Comparative analysis of temperature attainment

Drawing parallels to our investigations with gold and silver nanoparticles, we examined the variations in attained temperatures among different simulated forms of copper nanostructures. Figure 6 showcases the distinct thermal profiles achieved by copper nanorods, nanoellipsoids, and nanospheres. The copper nanorod, for instance, resulted in a maximum temperature of 43.3 °C, while the copper nanosphere and nanoellipsoid achieved a same temperature of 42.2 °C. These values, akin to our previous findings, were extracted from the particle centers and propagated into the surrounding medium. The thermal field spread of a copper nano-ellipsoid is greater than that of a copper nano-sphere or rod figure 6(b).

The exceptional thermal conductivity of gold can be aptly articulated through Fourier's Law ($q = -k\nabla T$). Here, 'q' denotes heat flux, 'k' stands for thermal conductivity and ∇T represents the temperature gradient. The prowess of gold in conducting heat efficiently ensures a swift dissipation of heat throughout the simulated environment, a pivotal factor in shaping the thermal dynamics of the nanoparticles. This fundamental understanding underscores our empirical observation that gold-coated copper nanoparticles exhibit enhanced heat-spreading capabilities, a crucial facet of hyperthermia applications.

3.3. Core–shell structure exploration: insights from gold nanoparticles study

To further enrich our exploration, we extended our analysis of core–shell structures to copper nanoparticles. Drawing inspiration from our study on gold nanoparticles, we investigated the effects of coating copper nanoparticles with different materials.

Just as with silver nanoparticles, we explored the impact of a shell made of Gold (Au) or PEG polymer on the heat dissipation process. Similar to our previous findings, the thermal conductivity coefficients of these simulated shell materials exhibited distinct trends, with gold displaying enhanced conductivity, as shown in figure 7. The temperature caused by the core of CuNPs was examined in this simulation by covering it with a shell of PEG polymer or Gold (Au). The effect of generated temperature on nanoparticle core is seen in figure 7(a) using varied shell thicknesses, as illustrated in figure 7(b). As seen in the graph, temperature decreases when the thickness of the Au shell increases and tends to rise as the size of the PEG polymer shell increases. Gold (Au) readily spreads heat to its surroundings due to its great thermal conductivity.

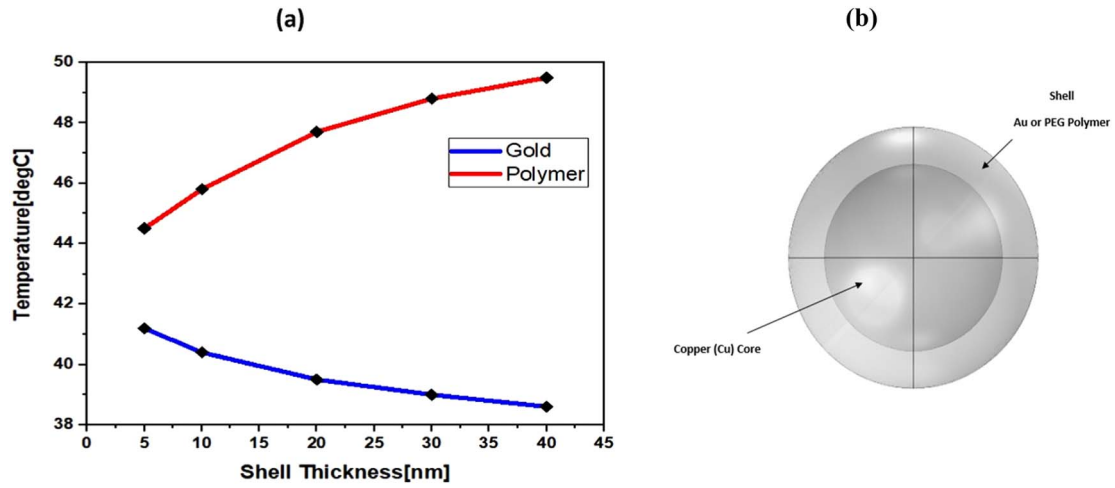

Figure 7. (a) Maximum temperature attained by superimposing Au and Polymer shells with thicknesses of 5 nm, 10 nm, 20 nm, 30 nm, and 40 nm. (b) The shell of the core structure.

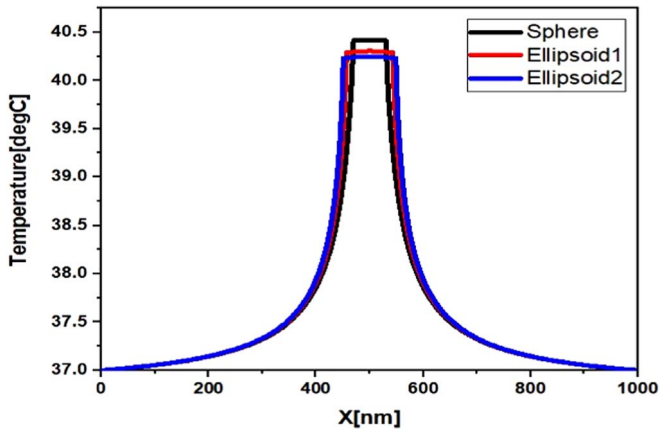

Figure 8. Different coating morphologies radial temperature distributions: 20 nm radius sphere, 1:25-25-43.2 nm ellipsoid-1, 2:22-25-49 nm ellipsoid-2.

3.4. Impact of coating surface and shape: lessons from gold nanoparticles study

Inspired by our investigations into irregular coating surfaces with gold nanoparticles, we examined the influence of different coating shapes on copper nanoparticles. Figure 8 presents a comparative analysis of temperature distributions for various surface coatings, including a spherical shell and two ellipsoids. Additionally, the temperature essential for hyperthermia is determined by the material and shell thickness, each of which is impacted by the specific position of application in the body.

Figure 8 clearly indicates that the temperature of the coated surface does not fluctuate substantially during the hyperthermia process, our study indicates that akin to gold nanoparticles, the anisotropy of coating surfaces might not play a significant role in the hyperthermia process for copper nanoparticles. These findings are in line with our observations from gold nanoparticles, emphasizing the marginal difference in temperature among different coating shapes.

Because of the unique characteristics of gold nanoparticles (AuNPs), they replicate and create tiny islands, which gradually expand into an imperfect and uneven covering, finally turning into a full shell encircling the center. Before being implanted in tissue with a radius of 500 nm, little AuNPs with a radius of 4 nm were connected to the surface of the core of CuNPs 20 nm radius. To describe the temperature distributions for improperly coated NPs with various numbers of NPs attached, the volume ratio of AuNPs relative to the entire shell volume was calculated, as shown in figure 9. The bare core body temperature inside the nanoparticles was 42.3 °C. The temperature showed a decreasing trend with an increase in the coating amount. The total shell temperature in the nanoparticle was measured about 40.6 °C. The maximum temperature attained by the core covered with different number of nanoparticles can be seen in table 2.

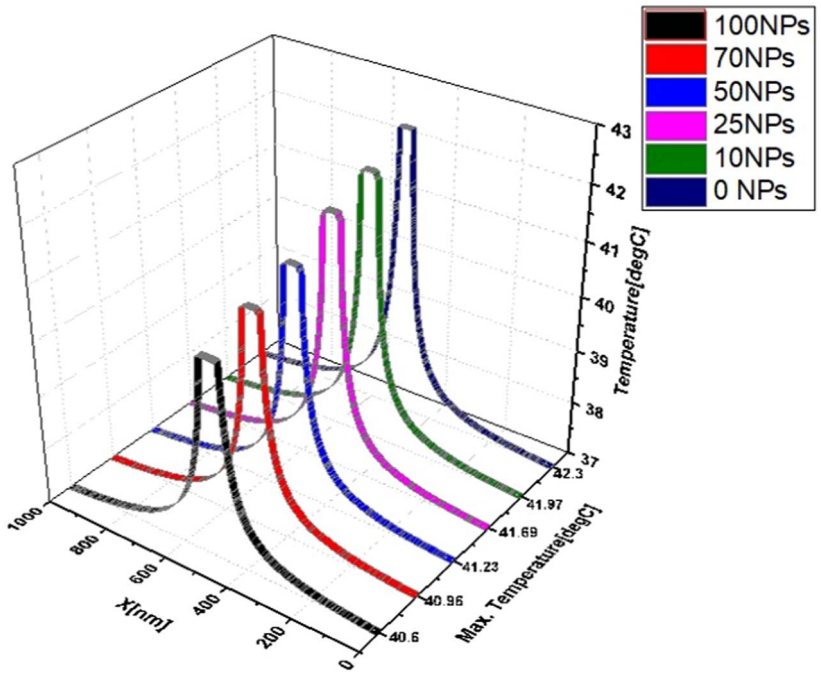

Figure 9. Radial thermal performance after 3 μs of heat treatment by varying the amount of surface coating.

Table 2. Temperature attained with different number of particles attached to the core.

No. of particles attached to core	0	10	25	50	70	100
T_{max} (°C)	42.3	41.97	41.69	41.23	40.95	40.6

The nanorods exhibited more heat than nanospheres, core–shell, and nanoellipsoids because nanorods have an elongated structure, leading to a more tunable localized surface plasmon resonance. Its anisotropic form is more suitable for light absorption and scattering than the other geometries. The sharp edges of nanorods also generate localized hotspots to maximize energy absorption rates.

4. Conclusions

Copper nanoparticles were chosen in this work because they are quasi, antimicrobial, and anti-bacterial, which seem to be important in hyperthermia applications. Nano-spheres, nano-rods, core-shells and nano-ellipsoids were employed in simulations that lasted 3 microseconds. Nano-rod obtained the maximum temperature (i.e., $T_{max} = 43.3$ °C) when compared to other forms. The therapeutic benefits of NP vary according to its size and shape. This research might improve the thermal efficiency of biomedical applications. The temperature field absorption rate of several types of NPs that had the same capacity was examined. Because of its higher thermal absorption rate, the copper nano-ellipsoid covered a larger center volume than other forms, with thermal equilibrium achieved after 0.5 μs from the beginning of the heating process. Thermal increment and decrement were explored in terms of thickness and form, and the thermal properties of the shell were revealed to govern thermal increment and decrement. Because of the thin shell, the noble metal core may attain its maximum temperature. The simulation looked at how varying gold shell covering volume ratios affected the heat sensitivity of a partly covered surface. Temperature variations affect the free surface left by the shell-forming process. Choice of materials, surface regularity, and surface coating depth are all essential considerations in using core–shell NPs, which comprise a noble metal core and a biocompatible surface.

Acknowledgments

The authors acknowledge the support from the Deanship of Scientific Research, Najran University. Kingdom of Saudi Arabia, for funding this work under the Research Groups funding program grant code number (NU/RG/SERC/12/15).

Data availability statement

All data that support the findings of this study are included within the article (and any supplementary files).

Conflict of interest

Authors declare no conflict of interest for publishing this work.

ORCID iDs

Muhammad Usama Daud https://orcid.org/0000-0002-6578-5019
Muhammad Yasin Naz https://orcid.org/0000-0002-8490-7819
Saifur Rahman https://orcid.org/0000-0002-7262-183X
Muawia Abdelkafi Magzoub Mohamed Ali https://orcid.org/0000-0002-3933-0221

References

[1] Lutgens L, van der Zee J, Pijls-Johannesma M, De Haas-Kock D F, Buijsen J, Mastrigt G A, Lammering G, De Ruysscher D K and Lambin P 2010 Combined use of hyperthermia and radiation therapy for treating locally advanced cervical carcinoma *Cochrane Database of Systematic Reviews* **20** CD006377
[2] Hegyi G, Szigeti G P and Szász A 2013 Hyperthermia versus oncothermia: cellular effects in complementary cancer therapy *Evidence-Based Complementary and Alternative Medicine* **2013** 672873
[3] Tabuchi Y, Wada S, Furusawa Y, Ohtsuka K and Kondo T 2012 Gene networks related to the cell death elicited by hyperthermia in human oral squamous cell carcinoma HSC-3 cells *Int. J. Mol. Med.* **29** 380–6
[4] Falk M H and Issels R D 2001 Hyperthermia in oncology *Int. J. Hyperth.* **17** 1–18
[5] Sharif-Khatibi L, Kariminia A, Khoei S and Goliaei B 2007 Hyperthermia induces differentiation without apoptosis in permissive temperatures in human erythroleukaemia cells *Int. J. Hyperth.* **23** 645–55
[6] Wust P, Hildebrandt B, Sreenivasa G, Rau B, Gellermann J, Riess H and Schlag P M 2002 Hyperthermia in combined treatment of cancer *Lancet Oncol.* **3** 487–97
[7] Van der Zee J 2002 Heating the patient: a promising approach? *Annals of Oncology* **13** 1173–84
[8] Rubio M F J C, Hernández A V and Salas L L 2013 High-temperature hyperthermia in breast cancer treatment *Hyperthermia. India* (InTech Publisher) 83–100
[9] Habash R W, Bansal R, Krewski D and Alhafid H T 2006 Thermal therapy, part 1: an introduction to thermal therapy *Crit. Rev. Biomed. Eng.* **34** 459–89
[10] Habash R W, Bansal R, Krewski D and Alhafid H T 2006 Thermal therapy, part 2: hyperthermia techniques *Crit. Rev. Biomed. Eng.* **34** 491–542
[11] Horsman M R and Overgaard J 2007 Hyperthermia: a potent enhancer of radiotherapy *Clinical Oncology* **19** 418–26
[12] Feldman A L, Libutti S K, Pingpank J F, Bartlett D L, Beresnev T H, Mavroukakis S M and Alexander H R 2003 Analysis of factors associated with outcome in patients with malignant peritoneal mesothelioma undergoing surgical debulking and intraperitoneal chemotherapy *Journal of Clinical Oncology* **21** 4560–7
[13] Stauffer P R 2000 Thermal therapy techniques for skin and superficial tissue disease *Matching the Energy Source to the Clinical Need: a Critical Review, Proceedings of SPIE* **102970E** 321–61
[14] Leonard Berlin M D 2004 Commentary: ACR practice guidelines and technical standards *Journal of the American College of Radiology* **1** 98–9
[15] Cheng K S and Roemer R B 2004 Optimal power deposition patterns for ideal high temperature therapy/hyperthermia treatments *Int. J. Hyperth.* **20** 57–72
[16] Prosnitz L R, Maguire P, Anderson J M, Scully S P, Harrelson J M, Jones E L and Brizel D M 1999 The treatment of high-grade soft tissue sarcomas with preoperative thermoradiotherapy *International Journal of Radiation Oncology* Biology* Physics* **45** 941–9
[17] Song C W, Patten M S, Chelstrom L M, Rhee J G and Levitt S H 1987 Effect of multiple heatings on the blood flow in RIF-1 tumours, skin and muscle of C3H mice *Int. J. Hyperth.* **3** 535–45
[18] Cavaliere R, Ciocatto E C, Giovanella B C, Heidelberger C, Johnson R O, Margottini M and Rossi-Fanelli A 1967 Selective heat sensitivity of cancer cells. Biochemical and clinical studies *Cancer* **20** 1351–81
[19] Haveman J, Van Der Zee J, Wondergem J, Hoogeveen J F and Hulshof M C C M 2004 Effects of hyperthermia on the peripheral nervous system: a review *Int. J. Hyperth.* **20** 371–91
[20] Walter P and Ron D 2011 The unfolded protein response: from stress pathway to homeostatic regulation *Science* **334** 1081–6
[21] Frey B, Weiss E M, Rubner Y, Wunderlich R, Ott O J, Sauer R and Gaipl U S 2012 Old and new facts about hyperthermia-induced modulations of the immune system *Int. J. Hyperth.* **28** 528–42
[22] Gehrmann M, Marienhagen J, Eichholtz-Wirth H, Fritz E, Ellwart J, Jäättelä M and Multhoff G 2005 Dual function of membrane-bound heat shock protein 70 (Hsp70), Bag-4, and Hsp40: protection against radiation-induced effects and target structure for natural killer cells *Cell Death & Differentiation* **12** 38–51
[23] Riley R S and Day E S 2017 Gold nanoparticle-mediated photothermal therapy: applications and opportunities for multimodal cancer treatment. *Wiley Interdiscip. Rev. Nanomed. Nanobiotechnol.* **9** e1449
[24] Kennedy L C, Bickford L R, Lewinski N A, Coughlin A J, Hu Y, Day E S, West J L and Drezek R A 2011 A new era for cancer treatment: gold-nanoparticle-mediated thermal therapies *Small* **7** 169–83
[25] Knight M W and Halas N J 2008 Nanoshells to nanoeggs to nanocups: optical properties of reduced symmetry core–shell nanoparticles beyond the quasistatic limit *New J. Phys.* **10** 105006
[26] Levin C S, Hofmann C, Ali T A, Kelly A T, Morosan E, Nordlander P, Whitmire K H and Halas N J 2009 Magnetic− plasmonic core–shell nanoparticles *ACS Nano* **3** 1379–88

[27] Loo C, Lin A, Hirsch L, Lee M H, Barton J, Halas N, West J and Drezek R 2004 Nanoshell-enabled photonics-based imaging and therapy of cancer *Technol. Cancer Res. Treat.* **3** 33–40
[28] Gobin A M, Lee M H, Halas N J, James W D, Drezek R A and West J L 2007 Near-infrared resonant nanoshells for combined optical imaging and photothermal cancer therapy *Nano Lett.* **7** 1929–34
[29] Qamar M *et al* 2022 Gold nanorods for doxorubicin delivery: numerical analysis of electric field enhancement, optical properties and drug loading/releasing efficiency *Materials* **15** 1764
[30] Day E S, Morton J G and West J L 2009 Nanoparticles for thermal cancer therapy *J. Biomech. Eng.* **131** 074001
[31] Sur S, Rathore A, Dave V, Reddy K R, Chouhan R S and Sadhu V 2019 Recent developments in functionalized polymer nanoparticles for efficient drug delivery system *Nano-Structures & Nano-Objects* **20** 100397
[32] Kumar K S, Kumar V B and Paik P 2013 Recent advancement in functional core–shell nanoparticles of polymers: synthesis, physical properties, and applications in medical biotechnology *Journal of Nanoparticles* **2013** 1–24
[33] Ai Y, Zhang F, Wang C, Xie R and Liang Q 2019 Recent progress in lab-on-a-chip for pharmaceutical analysis and pharmacological/toxicological test *TrAC, Trends Anal. Chem.* **117** 215–30
[34] Chen K, Wang C, Peng Z, Qi K, Guo Z, Zhang Y and Zhang H 2020 The chemistry of colloidal semiconductor nanocrystals: From metal-chalcogenides to emerging perovskite *Coord. Chem. Rev.* **418** 213333
[35] Bhattacharya P T, Misra S R and Hussain M 2016 Nutritional aspects of essential trace elements in oral health and disease: an extensive review *Scientifica* **2016** 5464373
[36] Siddiqui M A, Alhadlaq H A, Ahmad J, Al-Khedhairy A A, Musarrat J and Ahamed M 2013 Copper oxide nanoparticles induced mitochondria mediated apoptosis in human hepatocarcinoma cells *PLoS One* **8** e69534
[37] Georgopoulos P G, Roy A, Yonone-Lioy M J, Opiekun R E and Lioy P J 2001 Environmental copper: its dynamics and human exposure issues *Journal of Toxicology and Environmental Health Part B: Critical Reviews* **4** 341–94
[38] Kim J S, Adamcakova-Dodd A, O'Shaughnessy P T, Grassian V H and Thorne P S 2011 Effects of copper nanoparticle exposure on host defense in a murine pulmonary infection model *Part. Fibre Toxicol.* **8** 1–14
[39] Ren G, Hu D, Cheng E W, Vargas-Reus M A, Reip P and Allaker R P 2009 Characterisation of copper oxide nanoparticles for antimicrobial applications *Int. J. Antimicrob. Agents* **33** 587–90
[40] Gawande M B, Goswami A, Felpin F X, Asefa T, Huang X, Silva R, Zou X, Zboril R and Varma R S 2016 Cu and Cu-Based Nanoparticles: Synthesis and Applications in Catalysis *Chemical Reviews* **116** 3722–811
[41] Sharma H, Mishra P K, Talegaonkar S and Vaidya B 2015 Metal nanoparticles: a theranostic nanotool against cancer *Drug Discovery Today* **20** 1143–51
[42] Stephen Z R and Zhang M 2021 Recent progress in the synergistic combination of nanoparticle-mediated hyperthermia and immunotherapy for treatment of cancer. *Adv. Healthcare Mater.* **10** 2001415
[43] Goel S, Chen F and Cai W 2014 Synthesis and biomedical applications of copper sulfide nanoparticles: from sensors to theranostics *Small* **10** 631–45
[44] Stöber W, Fink A and Bohn E 1968 Controlled growth of monodisperse silica spheres in the micron size range *J. Colloid Interface Sci.* **26** 62–9
[45] Daud M U *et al* 2022 Finite element analysis of silver nanorods, spheres, ellipsoids and core–shell structures for hyperthermia treatment of cancer. *Materials* **15** 1786
[46] Abbas G, Maqbool S, Shahzad M K, Afzaal M, Daud M U, Fatima N G and Ghuffar A 2022 Analysis of gold nanospheres, nano ellipsoids, nanorods, and effect of core–shell structures for hyperthermia treatment. *RSC Adv.* **12** 9292–8
[47] Charny C K 1992 Mathematical models of bioheat transfer *Advances in Heat Transfer* **22** 19–155
[48] Pennes H H 1948 Analysis of tissue and arterial blood temperatures in the resting human forearm *J. Appl. Physiol.* **1** 93–122
[49] Ng E K and Sudharsan N M 2001 Effect of blood flow, tumour and cold stress in a female breast: A novel time-accurate computer simulation *Proc. Inst. Mech. Eng.* H **215** 393–404
[50] Kim D H, Nikles D E and Brazel C S 2010 Synthesis and characterization of multifunctional chitosan-MnFe2O4 nanoparticles for magnetic hyperthermia and drug delivery *Materials* **3** 4051–65
[51] Taloub S, Hobar F, Astefanoaei I, Dumitru I and Caltun O F 2016 FEM Investigation of coated magnetic nanoparticles for hyperthermia *J. Nanosci. Nanotechnol.* **6** 55–61
[52] Govorov A O, Zhang W, Skeini T, Richardson H, Lee J and Kotov N A 2006 Gold nanoparticle ensembles as heaters and actuators: melting and collective plasmon resonances *Nanoscale Res. Lett.* **1** 84–90
[53] Maina M R, Okamoto Y, Inoue R, Nakashiba S-ichi, Okada A and Sakagawa T 2018 Influence of surface state in micro-welding of copper by Nd:YAG laser *Applied Sciences* **8** 2364